Vol. 671: 97–110, 2021
https://doi.org/10.3354/meps13784

MARINE ECOLOGY PROGRESS SERIES
Mar Ecol Prog Ser

Published August 5

Mechanism for the marked increase of *Ulva prolifera* in the south Yellow Sea: role of light intensity, nitrogen, phosphorus, and co-limitations

Changyou Wang[1,*,#], Chen Chen[1], Rongguo Su[2], Zhuhua Luo[1,3], Longjiang Mao[1,#], Yuanzhi Zhang[1]

[1]School of Marine Sciences, Nanjing University of Information Science and Technology, Nanjing 210044, PR China
[2]Key Laboratory of Marine Chemistry Theory and Technology, Ministry of Education, Ocean University of China, Qingdao 266100, PR China
[3]Key Laboratory of Marine Biogenetic Resources, Third Institute of Oceanography, Ministry of Natural Resources, Xiamen 361005, PR China

ABSTRACT: An understanding of regulating factors and early warning of *Ulva prolifera* biomass increase may reduce harm or prevent bloom disasters in the Yellow Sea. We investigated the minimum nutrient concentration and light-limiting depth (Z_{lim}) for the growth of floating *U. prolifera* thalli. Bioavailable dissolved nitrogen (BDN) concentrations in most parts of the study area were almost always higher than the minimum N concentrations required for the growth of floating thalli, indicating no N limitation for the growth of floating thalli. However, the minimum N concentration required for the development of germlings into thalli was higher than BDN in the majority of the area north of 35° N. This indicated that germlings floating out of Subei Shoal were unable to grow into thalli because of N limitation. The minimum P concentration required for germling development was higher than the total dissolved P north of 35° N. This suggested that P limitation occurred for germlings floating out of Subei Shoal. The Z_{lim} for the floating thalli was <0.1 m in most parts of Subei Shoal, which explained why the rapid growth of floating thalli only occurred when they floated out from the Subei Shoal. A grid pattern with the phased multiple increase in biomass per day was designed to predict the possible accumulated multiple increase in biomass (AcMp) when *U. prolifera* drifted northward following different trajectories. The predicted AcMp values in 2017, 2010, and 2009 were close to the ratio of the coverage area from remote sensing data. Such a grid pattern facilitates quick decisions in disaster prevention and reduction.

KEY WORDS: *Ulva prolifera* · Nutrient limitation · Light limitation · Limiting depth · Effect interplay

1. INTRODUCTION

Green tides have occurred worldwide with increasing frequency during the last few decades (Valiela et al. 1997, Kamer et al. 2001, Hiraoka et al. 2004, Chávez-Sánchez et al. 2018) and have manifested themselves in the southern Yellow Sea since the summer of 2007 (Liu et al. 2009, Zhou et al. 2015, Song et al. 2019). *Ulva prolifera* is the dominant green tide species, forming large-scale macroalgal blooms in this area (Wang et al. 2015, Zhou et al. 2015). As an important mechanism supporting the formation of green tides, *U. prolifera* is an opportunistic species that is distributed worldwide, and has a complex life history, multiple reproduction modes, and a high reproductive rate (Kapraun 1970, Hiraoka et al. 2004, Lin et al. 2008). Diverse evidence, including satellite images, field observations, and physical oceanographic modeling, supports the original source of green algae on aquacultural rafts, which were inten-

*Corresponding author: chy.w@hotmail.com
#These authors contributed equally to this work

sively used in the *Porphyra yezoensis* culture industry, in the intertidal zone between 32° and 34° N (Liu et al. 2009, Zhou et al. 2015). Subei Shoal has been highlighted in previous studies on the formation mechanisms and the early development of green tides in the Yellow Sea (Wang et al. 2015, Zhou et al. 2015).

U. prolifera patches in the Yellow Sea, formed in the inshore waters of Jiangsu Province, drift northeastward due to interactions between wind and currents and subsequently increase in biomass, expand their coverage, and develop into large-scale blooms of green macroalgae along the coast of Shandong Peninsula, China (Wang et al. 2015, Song et al. 2019). The question arises of what key limiting factors prohibit *U. prolifera* blooms from occurring north of 34° N, but not at their presumed place of origin. More knowledge about bloom formation in this species is necessary. In particular, A clear understanding regarding the increasing biomass of *U. prolifera* is required to elucidate its formation mechanism, to discriminate key limiting factors, and to predict the sizes of green tides along their drift path. Although ecological factors influencing *U. prolifera* growth, including the supply of nutrients, light intensity, temperature, and competition with microalgae, have been studied previously (Solidoro et al. 1997, Luo et al. 2012, He et al. 2013, Risén et al. 2013, Wu 2013, Ren et al. 2014, Lamb 2018, Wang et al. 2019, 2020), an explicit and efficient method of coupling different ecological factors to estimate the growth of *U. prolifera* and to identify key limiting factors during its northward drift is lacking. The objectives of the present study were therefore to (1) elucidate the spatial differences in nutrient dynamics for large-scale blooms of macroalgae, especially *U. prolifera*; (2) identify the differences in N, P, and light intensity requirements between *U. prolifera* thalli and germlings; (3) reveal the formation mechanism of green tides and the key limiting factor(s) in the southern Yellow Sea; and (4) predict increases in *U. prolifera* biomass along a northward drifting trace. This work not only contributes to the early prevention of *U. prolifera* blooms, but also improves the ability to quickly react to green tide disasters.

2. MATERIALS AND METHODS

2.1. Investigation and measurement of seawater quality parameters

Samples to measure seawater quality parameters were collected in the southern Yellow Sea (32.0°–36.2° N, 120°–122.8° E) in late April 2017, 2018, and 2019 (Fig. 1). The collected surface water samples were filtered through pre-combusted (460°C for 6 h)

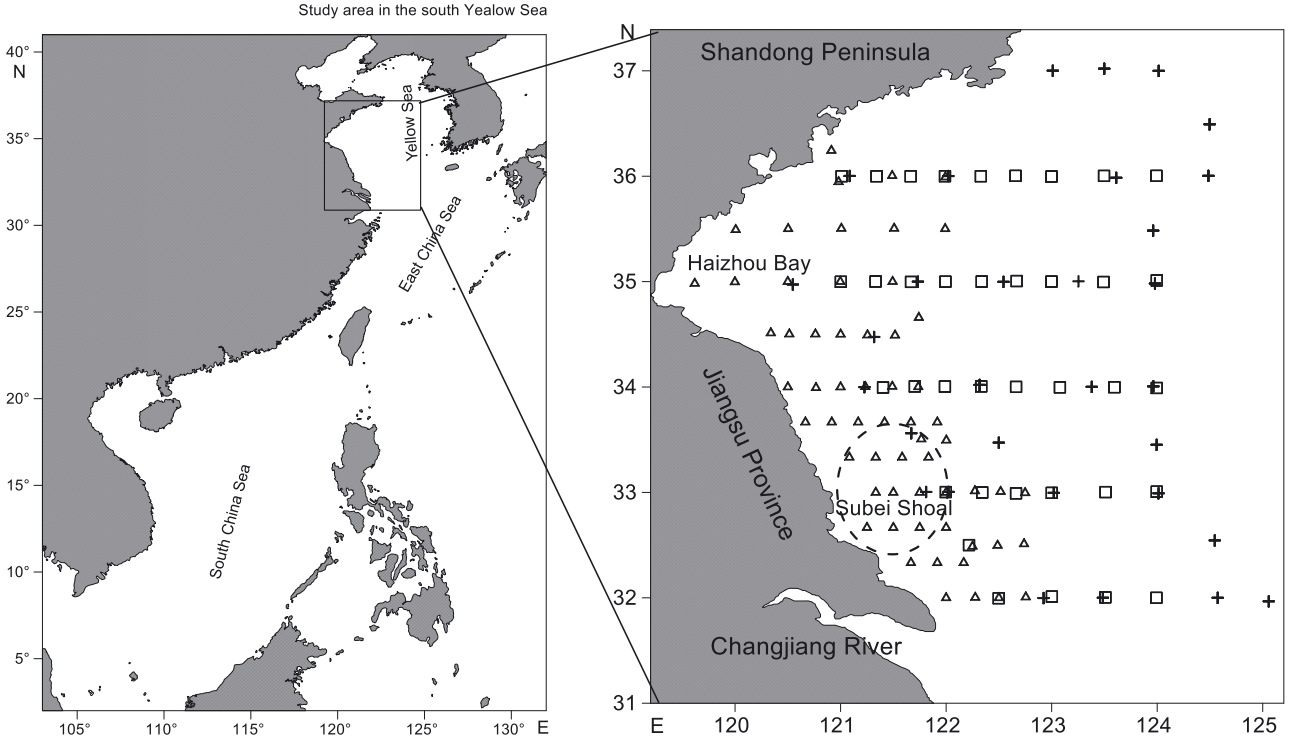

Fig. 1. Regional location and investigation area in the southern Yellow Sea. (△: sampling stations in April 2017; □: sampling stations in April 2018; +: sampling stations in April 2019; dashed ellipse: range of Subei Shoal)

0.45 µm GF/F filters (Millipore). Approximately 100 ml of filtrate from each sample were collected and stored at –20°C for subsequent measurements of dissolved N and P. The filtered samples were dried to a constant weight at 60°C and then re-weighed to determine the suspended particulate matter (SPM) concentration. Dissolved N and P concentrations were measured using a continuous flow autoanalyzer system (AAIII, Bran+Luebbe). NO_3^- concentrations were measured using the cadmium–copper reduction method, NO_2^- concentrations were measured using the standard pink azo-dye method, and NH_4^+ concentrations were measured using the indophenol blue method (Grasshoff et al. 2007). Dissolved inorganic nitrogen (DIN) is the sum of nitrate, nitrite, and ammonium concentrations. Dissolved inorganic phosphorus (DIP, PO_4^{3-}-P) concentrations were determined using the molybdate blue method (Grasshoff et al. 2007). Total dissolved nitrogen (TDN) and total dissolved phosphorus (TDP) were determined using the same method as DIN and DIP, except for the use of acid persulfate oxidation (Grasshoff et al. 2007). Dissolved organic nitrogen (DON) is the difference between TDN and DIN, and dissolved organic phosphorus (DOP) is the difference between TDP and DIP. Chlorophyll *a* (chl *a*) fluorescence was measured using a multi-parameter YSI (EXO) sonde with the 6025 chlorophyll sensor placed *in situ*. The values of the parameters (DIN, DON, DIP, DOP, SPM, and chl *a*) for samples collected from 60, 37, and 34 stations in late April 2017, 2018, and 2019, respectively, were measured and gridded by a Kriging method with a square of 0.1° × 0.1° N latitude and E longitude (Fig. 1). The data from each grid in the 3 years were averaged and used to calculate the growth of *Ulva prolifera* in the present study.

2.2. Light intensity for the growth of *U. prolifera*

The relationship between light intensity and water depth can be described using the following formula (Lalli & Parsons 1993):

$$L = L_0 \exp(-K \times Z) \quad (1)$$

where Z is the depth of the water column (m), K is the diffuse attenuation coefficient (m^{-1}), L is the light intensity (W m^{-2}) as a decreasing function of Z, and L_0 is the incident light intensity of the water surface (W m^{-2}), which can be calculated using solar radiation information obtained from the literature (Kalnay et al. 1996, Kistler et al. 2001).

In the present study, K was partitioned as follows (Kelble et al. 2005):

$$K = K_{sw} + K_{CDOM} + K_{chl} + K_{tripton} = 0.0384 + 0.000424 \times C_{CDOM} + 0.014 \times C_{chl} + (0.296 + 0.0492 \times C_{tripton}) \quad (2)$$

where K_{sw} is the partial attenuation coefficient for seawater and is usually assumed to be 0.0384 m^{-1} (Lorenzen 1972), K_{CDOM} is the partial attenuation coefficient for chromophoric dissolved organic matter (CDOM) and increases with CDOM concentration (quinine sulfate units), K_{chl} is the partial attenuation coefficient for chl *a* and increases with C_{chl} (a measure of phytoplankton abundance, mg m^{-2}). $K_{tripton}$ is the partial attenuation coefficient for tripton and increases with SPM (mg l^{-1}) (Kelble et al. 2005).

2.3. Method for analyzing light intensity and nutrient limitations

Bloom-forming *U. prolifera* is highly branched and composed of hollow tubular thalli with monochromatic walls that float in surface water (X. Zhang et al. 2008, Luo et al. 2012, B. Zhang et al. 2012, Zhou et al. 2015). The floating thalli of *U. prolifera* are generally shorter than 0.35 m. Assuming that macroalgal cells with abundant carrier proteins can bind with the nutrient molecules to form surface complexes, a transmembrane transport of nitrate or phosphate can be described as a surface complexation reaction. When the reaction instantaneously reaches equilibrium with the environmental concentration of the nutrient, a macroalgal growth equation with nutrient effects (Eq. 3) is established based on the von Bertalanffy growth equation and a nutrient absorption model can be constructed from the transmembrane transport of nitrate or phosphate (von Bertalanffy 1951, Wang et al. 2019):

$$\frac{dV}{dt} = \frac{\mu^a_{max}[NP]}{K_M + [NP]} V^m - kV \quad (3)$$

where V is the volume of the organism, t is time, [NP] is the nutrient (nitrogen or phosphorus) concentration, K_M is the conditional stability constant of the complexation reaction and is the concentration at half-speed, m is the effective coefficient of the absorption area of the nutrients, μ^a_{max} is the maximum absorption parameter regarding the absorption rate of nutrients and is termed the intrinsic growth rate, and k is the dissimilation rate per unit volume (Wang et al. 2019) (Table 1).

However, when nutrients are replete in the environment, the assimilation rate of nutrients, determined by the amount of specific activated enzymes (Chen 2015), regulates the uptake of nutrients in

Table 1. Main terms and abbreviations used in this study

Abbreviation	Description	Unit
V	Volume of the organism	mg l^{-1}
k	Dissimilation rate per unit volume	d^{-1}
μ^a_{max}	Maximum absorption parameter regarding the absorption rate of nutrients	d^{-1}
m	Effective coefficient of the absorption area of the nutrients	
K_M	Nutrient concentration at half-speed	µmol l^{-1}
K_a	Light intensity at half-speed	W m^{-2}
[NP]	Nutrient (nitrogen or phosphorus) concentration	µmol l^{-1}
[L]	Light intensity	W m^{-2}
$[Min\_NP]_{gm}$	Minimum concentration of nutrients for germlings to develop into thalli when light intensity is sufficient	µmol l^{-1}
$[Min\_N]_{gm}$	Minimum nitrogen concentration for germlings to develop into thalli when light intensity is sufficient	µmol l^{-1}
$[Min\_P]_{gm}$	Minimum phosphorus concentration for germlings to develop into thalli when light intensity is sufficient	µmol l^{-1}
$[Min\_L]_{gm}$	Minimum light intensity for germlings to develop into thalli when concentration of nutrients is sufficient	W m^{-2}
$[Min\_NP]_g$	Minimum concentration of nutrients for germlings to develop into thalli at a given light intensity	µmol l^{-1}
$[Min\_N]_g$	Minimum nitrogen concentration for germlings to develop into thalli at a given light intensity	µmol l^{-1}
$[Min\_P]_g$	Minimum phosphorus concentration for germlings to develop into thalli at a given light intensity	µmol l^{-1}
$[Min\_L]_g$	Minimum light intensity for germlings to develop into thalli at a given concentration of nutrients	W m^{-2}
$[Min\_NP]_f$	Minimum concentration of nutrients for floating thalli growth at a given light intensity	µmol l^{-1}
$[Min\_N]_f$	Minimum nitrogen concentration for floating thalli growth at a given light intensity	µmol l^{-1}
$[Min\_P]_f$	Minimum phosphorus concentration for floating thalli growth at a given light intensity	µmol l^{-1}
$[Min\_L]_f$	Minimum light intensity for floating thalli growth at a given concentration of nutrients	W m^{-2}
Z_{limf}	Critical (limiting) depth below which floating thalli cannot grow	m
Z_{limg}	Critical (limiting) depth below which germlings cannot grow	m
n	Photon amount in the activation of a specific enzyme	
Mp	Multiple increase in biomass of *U. prolifera*	
AcMp	Accumulated multiple of increase in biomass of *U. prolifera*	
AvMpd	Average multiple of increase in biomass of *U. prolifera* per day	d^{-1}
Mpd	Multiple of increase in biomass of *U. prolifera* per day	d^{-1}

macroalgal cells (Touchette & Burkholder 2000, González-Galisteo et al. 2019). Assuming such activation of specific enzymes follows an energy transition reaction, the growth model for macroalgae with light effect can be mathematically expressed by Eq. (4), following Eq. (3) (Wang et al. 2019):

$$\frac{dV}{dt} = \frac{\mu^a_{max}[L]^n}{K_a^n + [L]^n} V^m - kV \quad (4)$$

where [L] is the light intensity, K_a is the light intensity at half-speed, and n is the photon amount in the activation of the specific enzyme (Table 1).

The growth limitation process of macroalgae abides by Liebig's law of the minimum, where one ecological factor is deficient and all others are sufficient (Ebelhar et al. 2008). When the response of macroalgae to various levels of a nutrient or light intensity is studied, the volumetric growth rate can be formulated as follows (Wang et al. 2020):

$$\frac{dV}{dt} = \min\left\{\frac{\mu^a_{max}[L]^n}{K_a^n + [L]^n} V^m - kV, \frac{\mu^a_{max}[NP]}{K_M + [NP]} V^m - kV, \ldots\right\} \quad (5)$$

The formula for this law has been mathematically expressed as the product of a series of factor effects (Lang 1924, Ebelhar et al. 2008). The improved Shelford's law of tolerance demonstrates that the range of tolerance of organisms to one of the ecological factors is decreased when another tolerance has been approached by another ecological factor, explaining the interplay between ecological factor effects (Shelford 1913, Odum & Barrett 2005, Wang et al. 2020). When nutrient and light intensity are deficient, the volumetric growth rate can be formulated accordingly as:

$$\frac{dV}{dt} = \min\left\{\frac{[L]^n}{K_a^n + [L]^n} \frac{[NP]}{K_M + [NP]} \mu^a_{max} V^m - kV, \frac{[NP]}{K_M + [NP]} \frac{[L]^n}{K_a^n + [L]^n} \mu^a_{max} V^m - kV, \ldots\right\} \quad (6)$$

The first 2 terms in the 'min' operator are equivalent and can be simplified. Eq. (6) shows that volumetric growth rate will increase with nutrients at a certain level of light intensity or increase with light intensity at a certain level of nutrients, but the actual volumetric growth rate is the minimum between the calculated value by nutrients and that by light intensity.

Eq. (3) describes the response of *U. prolifera* to various nutrient levels (Wang et al. 2019). The effective coefficient of the nutrient absorption area of *U. prolifera*, m, decreases with increasing *U. prolifera* density. In the normal floating state of the alga, m could be a stable value, but m trends to 1 when algal volume becomes very small. That is, when $V \to 0$, $m \to 1$

at the same time. When Eq. (3) is equal to 0, and $V \to 0$ and $m \to 1$, the minimum concentration of nutrients for germlings to develop into thalli ($[\text{Min\_NP}]_{gm}$) can be deduced using the following formula:

$$[\text{Min\_NP}]_{gm} = \frac{K_M \cdot k}{\mu_{max}^a - k} \quad (V \to 0; m \to 1) \tag{7}$$

$[\text{Min\_NP}]_{gm}$ can be used to predict the development and occurrence of green tides caused by *U. prolifera* in coastal waters.

Similarly, Eq. (4) describes the response of *U. prolifera* to various light intensity levels (Wang et al. 2020). When Eq. (4) is equal to 0, and $V \to 0$ and $m \to 1$, the light intensity limit for the development of germlings of macroalgae ($[\text{Min\_}L]_{gm}$) can be obtained:

$$[\text{Min\_}L]_{gm} = K_a\left(\frac{k}{\mu_{max}^a - k}\right)^{\frac{1}{n}} \quad (V \to 0; m \to 1) \tag{8}$$

$[\text{Min\_}L]_{gm}$ can be used to elucidate the impossibility of germlings developing into thalli in highly turbid waters regardless of the nutrient concentration. This is very important for explaining the path development of *U. prolifera* in the southern Yellow Sea. A limiting value of 40 W m^{-2} has previously been determined for the development of germlings (Wang et al. 2020).

Eq. (6) shows that the parameters of the potential volume function depend on the levels of ecological factors regulating growth. When nutrients (N or P) and light intensity play a key role in *U. prolifera* growth and all other ecological factors are maintained at non-limiting levels (Li 2015, Gao et al. 2016, Wang et al. 2019, 2020), a growth equation coupling nutrient concentration and light intensity effects can be established to construct the relationship between the limiting ecological factors (Eq. 9) (Wang et al. 2020):

$$\frac{dV}{dt} = \frac{[L]^n}{K_a^n + [L]^n} \frac{[\text{NP}]}{K_M + [\text{NP}]} \mu_{max}^a V^m - kV \tag{9}$$

When Eq. (9) equals zero, the minimum light intensity for the growth of floating thalli ($[\text{Min\_}L]_f$) is obtained at a specific nutrient concentration:

$$[\text{Min\_}L]_f = K_a\left(\frac{kV^{1-m}}{\frac{[\text{NP}]}{K_M + [\text{NP}]}\mu_{max}^a - kV^{1-m}}\right)^{\frac{1}{n}} \tag{10}$$

As shown in Eq. (10), $[\text{Min\_}L]_f$ is regulated by [NP] and V, which elucidates the influence of *U. prolifera* density and nutrient concentration on the effect of light. $[\text{Min\_}L]_f$ increases with decreasing [NP] at a stable density of *U. prolifera* in green tides.

As $V \to 0$ and $m \to 1$ in Eq. (10), the minimum light intensity for germlings to develop into thalli ($[\text{Min\_}L]_g$) can be deduced using the following formula:

$$[\text{Min\_}L]_g = K_a\left(\frac{k}{\frac{[\text{NP}]}{K_M + [\text{NP}]}\mu_{max}^a - k}\right)^{\frac{1}{n}} \tag{11}$$

$[\text{Min\_}L]_g$ is regulated by [NP] and decreases with increasing [NP], which explains the interplay between $[\text{Min\_}L]_g$ and [NP] and the complementarity of ecological factors. When [NP] is large enough to be an unrestricted factor, $[\text{Min\_}L]_g$ converges toward $[\text{Min\_}L]_{gm}$.

When replacing L with $[\text{Min\_}L]_f$ and $[\text{Min\_}L]_g$, the limiting depths for floating thalli (Z_{limf}) and germlings (Z_{limg}) can be calculated using Eq. (1):

$$Z_{lim} = \frac{\ln L_0 - \ln L}{K} \tag{12}$$

Z_{limf} (or Z_{limg}) is the critical depth below which thalli (or germlings) cannot grow. This can be used as a clear manifestation of why the majority of thalli (or germlings) cast from *Porphyra yezoensis* culture rafts could not grow even in shallow waters in the Subei Shoal.

We can also derive from Eq. (9) the minimum nutrient concentration for floating thalli ($[\text{Min\_NP}]_f$) growth and the minimum nutrient concentration for germling development ($[\text{Min\_NP}]_g$) when $V \to 0$ and $m \to 1$:

$$[\text{Min\_NP}]_f = \frac{K_M k V^{1-m}}{\frac{[L]^n}{K_a^n + [L]^n}\mu_{max}^a - kV^{1-m}} \tag{13}$$

$$[\text{Min\_NP}]_g = \frac{K_M k}{\frac{[L]^n}{K_a^n + [L]^n}\mu_{max}^a - k} \tag{14}$$

$[\text{Min\_NP}]_f$ is regulated by $[L]$ and V, which shows the influence of *U. prolifera* density and light intensity on the nutrient effect. $[\text{Min\_NP}]_f$ increases with decreasing $[L]$ at a stable density of *U. prolifera* in the green tide. $[\text{Min\_NP}]_g$ is only regulated by $[L]$ and decreases with increasing $[L]$. When $[L]$ is large enough to be an unrestricted factor, $[\text{Min\_NP}]_g$ converges toward $[\text{Min\_NP}]_{gm}$.

2.4. Determining the path of floating *U. prolifera* and calculating the multiple increase in biomass in the grid area

The satellite tracking and coverage of *U. prolifera* were calculated with MODIS-TERRA data and presented by North China Sea Marine Forecasting Center. For simplicity and conciseness, a centroid tracking algorithm was used to determine the trace of floating *U. prolifera* (Wang et al. 2009). The area of the floating *U. prolifera* was first divided into n small

Table 2. Estimated drift velocities and the time that *Ulva prolifera* passed through a grid during May and July in the present study. V_d: drift velocity; T_e: estimated time through a grid (single values are means and double values are ranges)

Date	Late May		Early June		Mid-June		Late June		Early July	
Direction	W	N	W	N	W	N	E	N	E	N
V_d (m s^{-1})	0.08	0.15	0.12	0.2	0.07	0.14	0.03	0.13	0.02	0.08
	0.06–0.1	0.1–0.2	0.1–0.14	0.15–0.25	0.04–0.1	0.1–0.18	0.01–0.05	0.1–0.16	0.01–0.03	0.06–0.1
T_e (d)	13	8	9	7	15	9	35	10	52	16
	11–18	6–13	8–11	5–9	11–26	7–13	21–105	8–13	35–105	13–21

triangles, and the centroid of every triangle was calculated as below:

$$x_j = \frac{\sum_{i=1}^{3} x_i}{3} \quad (15)$$

$$y_j = \frac{\sum_{i=1}^{3} y_i}{3} \quad (16)$$

where points (x_i, y_i) (i = 1, 2, 3) are the vertex coordinates of a small triangle, and points (x_j, y_j) (j = 1–n) are the centroids of the small triangles. The above process was then repeated until only 1 point was obtained.

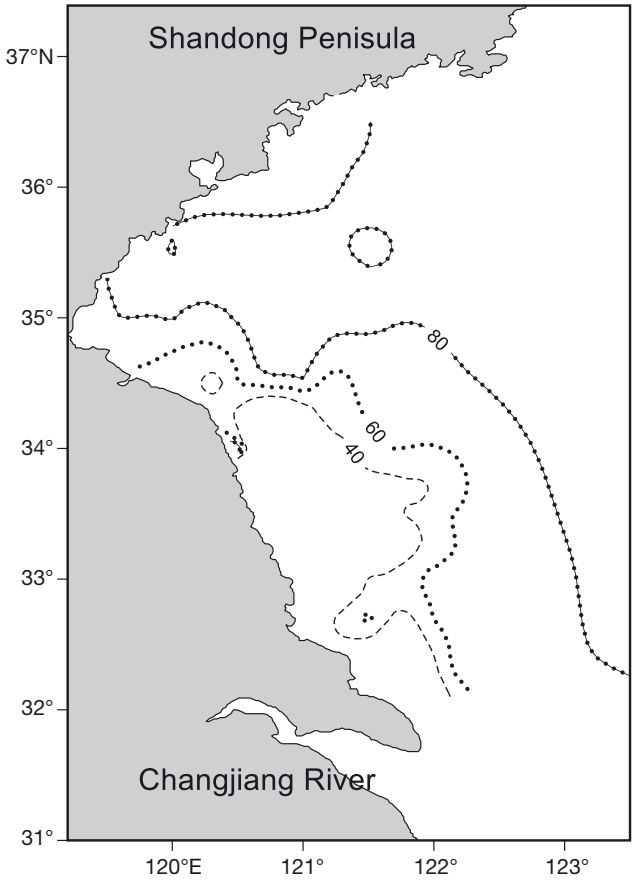

Fig. 2. Average light intensities (W m^{-2}) in April in the surface seawater layer above 0.35 m in the southern Yellow Sea (calculated from the diffuse attenuation coefficient and solar radiation) (solid-circle line: 80 W m^{-2}; dotted line: 60 W m^{-2}; dashed line: 40 W m^{-2})

The trace of *U. prolifera* drifting northward often moves in the range of 120° to 122.5° E because of variable hydrodynamics (Huang et al. 2014), and can be divided into 3 pathways: west, middle, and east path. The relative sea area, located from 32.5° N to the southern sea area along Shandong Peninsula, and from 119.5° to 123.5° E were divided into 57 grids with a square of 0.5° × 0.5° N latitude and E longitude. The growth rate of *U. prolifera* in each grid was calculated using Eq. (9), based on the distribution of nutrients, light intensity, and Z_{limf}. The corresponding multiple increase in biomass per day (Mpd) in these grids was obtained from the growth rate of *U. prolifera* plus 1. When *U. prolifera* drifted through the grids, its increase in biomass was calculated with Mpd to the power of residence time (t).

As reported previously, the drift velocities of *U. prolifera* in different months have been estimated based on satellite remote sensing images and ocean models (Yi et al. 2010, Xia 2016). The time of *U. prolifera* passing through a grid (T_e) was estimated from the drift with *U. prolifera* velocities (Table 2). Here, half of T_e was only applied when *U. prolifera* went in or out of (did not pass through) the grid. Then, t was obtained from the accumulation of T_e. Using Mpd and t, accumulated Mp (AcMp) was predicted to prevent and control *U. prolifera* green tide formation for management purposes.

3. RESULTS AND DISCUSSION

3.1. Distribution of light intensity in seawater and the corresponding minimum nutrient concentrations for *Ulva prolifera* growth in the south Yellow Sea

Using Eq. (1), the average light intensity (ALIN) in the seawater column from 0 to 0.35 m was calculated to analyze the growth of *U. prolifera*. As shown in Fig. 2, ALIN was strong from the head of Haizhou Bay to the open waters of the southern Yellow Sea,

with a value >80 W m^{-2}. South of 35° N, ALIN decreased gradually from north to south and was <40 W m^{-2} in the Subei Shoal. In contrast, ALIN retained a value >80 W m^{-2} in most areas north of 35° N. Nevertheless, the field ALIN is higher than the intensity of inhibition in most parts of the study area (Wang et al. 2020). Eq. (9) primarily focused on growth of *U. prolifera* from an ecological perspective. Therefore, compensation intensity of light in physiology is not taken into consideration in this study.

Using Eq. (14), the minimum N concentration required for the development of germlings ($[Min\_N]_g$) was calculated to be 8.5 and 7.0 µmol l^{-1} at ALINs of 60 and 80 W m^{-2}, respectively (Fig. 3). The minimum P concentration for the development of germlings ($[Min\_P]_g$) was 0.35 and 0.29 µmol l^{-1} at ALINs of 60 and 80 W m^{-2}, respectively. The minimum N concentration for the growth of floating thalli ($[Min\_N]_f$) was calculated based on Eq. (13), yielding values of 3.1, 2.0, and 1.9 µmol l^{-1} at ALINs of 40, 60, and 80 W m^{-2}, respectively (Fig. 3c). The minimum P concentration for the growth of floating thalli ($[Min\_P]_f$) was calculated to be 0.13, 0.086, and 0.078 µmol l^{-1} at ALINs of 40, 60, and 80 W m^{-2}, respectively (Fig. 3d). $[Min\_N]_g$ and $[Min\_P]_g$ were much larger than the corresponding $[Min\_N]_f$ and $[Min\_P]_f$. A possible explanation is that germlings cannot store large amounts of nutrients when nutrients are abundant and will not survive when nutrients are lacking (Lamb 2018). Fig. 3 demonstrates that the distribution of ALIN determines the distribution of the minimum nutrient concentration for the development of germlings and the growth of floating thalli.

3.2. Average distribution of dissolved nutrients available for *U. prolifera* growth in the south Yellow Sea

In April, average DIN decreased from south to north (Fig. 4), indicating coastal DIN input combined with that from Changjiang River, particularly from the intensive input of DIN around the estuary of the obsolete Yellow River. In the largest part of the sea area north of 35° N, DIN was <1.9 µmol l^{-1}, which was less than both $[Min\_N]_f$ and $[Min\_N]_g$ and is an inexorable trend of N limitation for floating thalli and germlings of *U. prolifera* in this area of the south Yellow Sea. However, this conclusion is inconsistent with the field investigation, which showed a slight increase in the biomass of *U. prolifera*. Therefore, more N species should be considered when an expla-

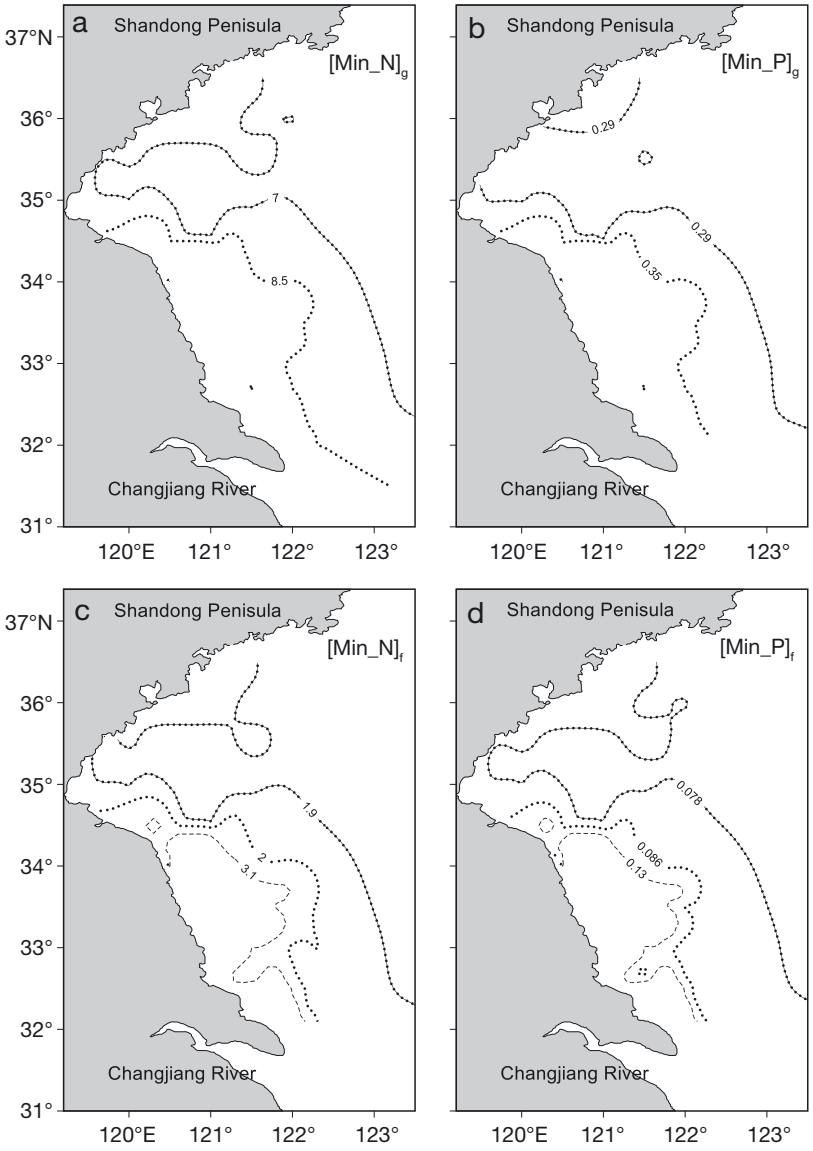

Fig. 3. Minimum nutrient concentrations (µmol l^{-1}) for (a,b) the development of germlings and (c,d) the growth of floating thalli of *Ulva prolifera* in the south Yellow Sea (different line styles indicate minimum concentrations calculated at different average light intensities as defined in Fig. 2). $[Min\_N]_g$ ($[Min\_P]_g$): minimum nitrogen (phosphorus) concentration required for germlings to develop into thalli; $[Min\_N]_f$ ($[Min\_P]_f$): minimum nitrogen (phosphorus) concentration to support the growth of floating thalli. Values for the solid-circle lines, dotted lines and dashed line are given in µmol l^{-1}

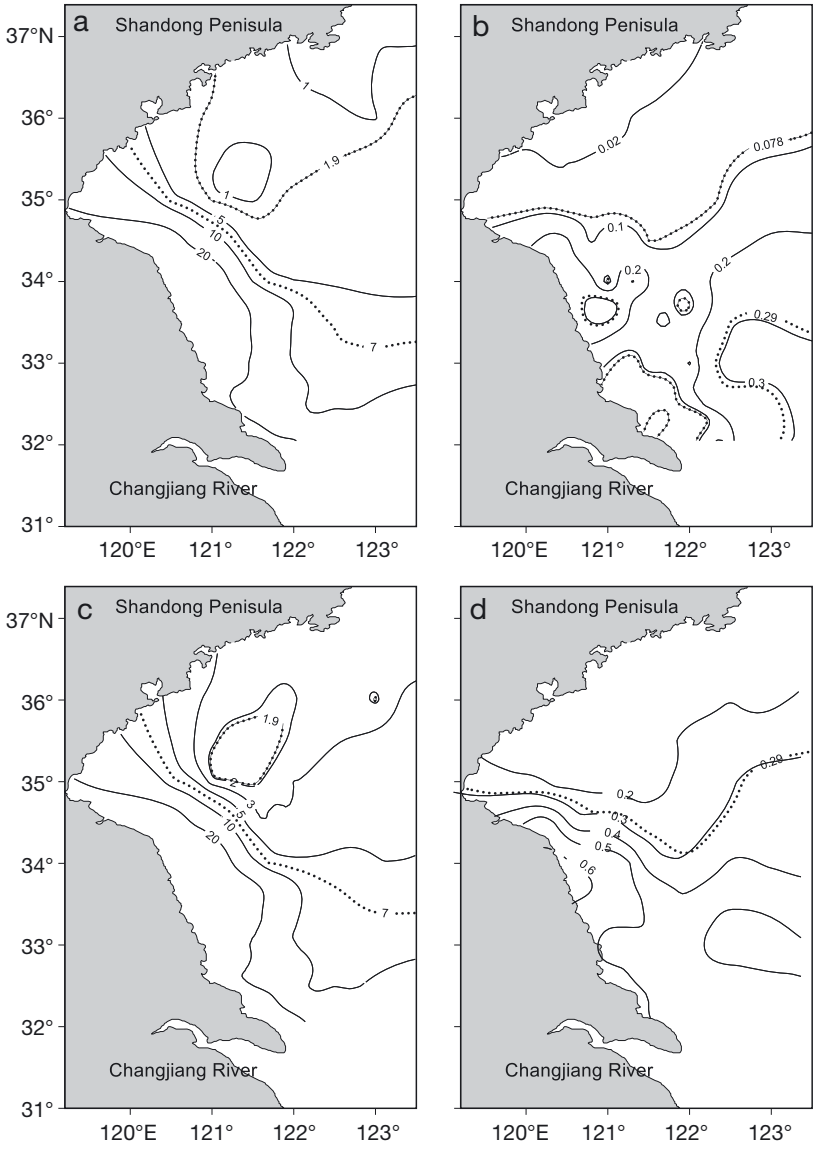

Fig. 4. Distribution of average (a) dissolved inorganic nitrogen (DIN), (b) dissolved inorganic phosphorus (DIP), (c) bioavailable dissolved nitrogen (BDN), and (d) total dissolved phosphorus (TDP) in the southern Yellow Sea in April 2017–2019. (Solid line: contour line of DIN, DIP, BDN or TDP; solid-circle line: concentration below which thalli cannot grow; dotted line: concentration below which germlings cannot grow). Values given in µmol l^{-1}

nation involving $[Min\_N]_f$ and $[Min\_N]_g$ is presented for the growth of *U. prolifera*.

DON of low molecular weight can be directly absorbed by organisms such as *U. prolifera* and should be taken into consideration in the growth of *U. prolifera*. Thus low-molecular-weight bioavailable DON is mainly composed of dissolved free amino acids (DFAA) and urea in the southern sea area of the Shandong Peninsula (Xiu et al. 2019, Jing 2020). Fig. 4 shows that the bioavailable dissolved nitrogen (BDN, defined as BDN = DIN + DFAA + urea) in the present study decreased from south to north, similar to DIN. Although the difference between BDN and DIN was only 0.85 µmol l^{-1}, it led to BDN values >1.9 µmol l^{-1} in the majority of the sea area north of 35° N. This indicated that N limitation seldom occurred in the study area, which is in agreement with previous investigations (Zhang et al. 2020).

DIN and BDN were both <7 µmol l^{-1}, which was lower than $[Min\_N]_g$ in the majority of the sea area above 34° N, except for the coast between 34° and 35° N. Therefore, the *U. prolifera* germlings floating out from Subei Shoal could not grow into thalli and could therefore not contribute to the green tide of *U. prolifera* due to N limitation. According to the BDN and ALIN, germlings settling on *Porphyra* farming rafts in Subei Shoal could find most favorable conditions. Therefore, it was the growth of thalli floating out from Subei Shoal rather than that of germlings that contributed to the marked increase in biomass and led to the formation of green tides of *U. prolifera* in the southern Yellow Sea.

Similarly, average DIP in April decreased from south to north (Fig. 4), indicating coastal DIP input combined with that from Changjiang River. Only DIP concentrations in the north of the estuary of the Changjiang River and the coastal waters (around 120.4° E, 34.3° N, which is the past estuary of the Yellow River) were higher than $[Min\_P]_g$ (0.29 µmol l^{-1}). Therefore, the thalli and germlings of *U. prolifera* floating into these 2 areas did not experience P limitation.

However, DIP in the majority of the sea area above 35° N was <0.078 µmol l^{-1}, which was lower than both $[Min\_P]_f$ and $[Min\_P]_g$. DIP in the Subei Shoal (ranging over 121°–122° E, 32.5°–33.5° N) was also <0.29 µmol l^{-1}, which was lower than $[Min\_P]_g$. Thus, P limitation occurred for both floating thalli and germlings of *U. prolifera* in the sea north of 35° N and for the development of germlings into thalli of *U. prolifera* in Subei Shoal. Here, an apparent paradox occurred because biomass of floating *U. prolifera* continued to increase in the area north of 35° N

based on the results of a previous study (Zhang et al. 2020), requiring more consideration of bioavailable P species in this area.

The velocity of P cycling varies over an extensive range, from several times per day to once per month, when the relative contribution of DIP to TDP ranges from 15 to 50% (Nausch & Nausch 2006, Zhang & Yin 2007, McLaughlin et al. 2013). *U. prolifera* produces phosphatase in P-limited environments (Sun et al. 2015), and phytoplankton and bacterioplankton are also activated to synthesize phosphatase in the dissolved phase due to P limitation (Chróst & Overbeck 1987, Labry et al. 2016). This could promote P cycling and might interfere with P uptake by *U. prolifera*. The residence time of dissolved P has been measured within a range of 3–4 d in the south Yellow Sea (Zhang & Yin 2007). Such a rapid turnover rate could sustain high primary production at a low DIP concentration. However, P limitation might continue to occur for floating thalli and germlings of *U. prolifera* in the southern sea area of Shandong Peninsula if P was cycled at a relatively low speed compared to the growth of *U. prolifera*. Previous studies have shown a decrease in *U. prolifera* biomass when they floated beyond 35.5° N (Huang et al. 2014, Guo et al. 2016), which likely resulted from the relatively low velocity of P cycling. In this case, TDP approximates the bioavailable dissolved P because DOP can be hydrolyzed to DIP with the catalysis of alkaline phosphatase (Huang et al. 2007, Baltar et al. 2016).

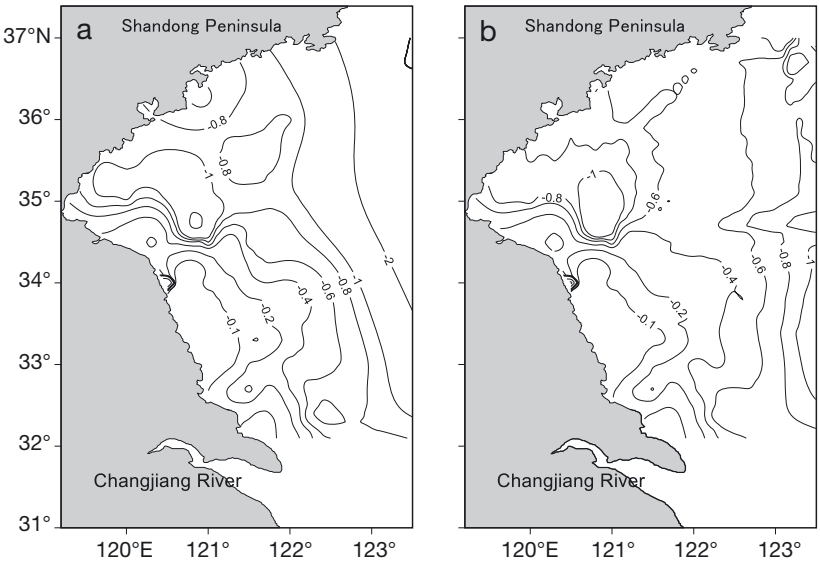

Fig. 5. Limiting depth (Z_{lim} in m) calculated for (a) floating thalli (Z_{limf}) and (b) germlings (Z_{limg}) of *Ulva prolifera* in the southern Yellow Sea in April 2017–2019, based on the minimum light intensities for the growth of thalli ($[L]_f$) and the growth of germlings ($[L]_g$)

3.3. Limiting depth for the growth of floating thalli and germlings of *U. prolifera*

The Z_{lim} in the study area was <2.0 m (Fig. 5), while the mixing layer in the Yellow Sea is lower than 10 m in Spring (Ge et al. 2006). This means that the mixing layer included the Z_{lim}. Water column mixing can enhance net primary productivity, replenish nutrients, and have an impact on phytoplankton succession, diversity, and similarity (Lindenschmidt & Chorus 1998, Jäger et al. 2008). Although the concentrations of nutrients in the Subei Shoal were the highest in the south Yellow Sea, the depth at which the minimum light intensity sustained the growth of floating thalli and germlings of *U. prolifera* was shallow owing to high turbidity. As shown in Fig. 5, Z_{limf}, the depth with a transmitted light intensity equal to $[Min\_L]_f$, was less than 0.1 m in most parts of the Subei Shoal. Therefore, floating thalli lower than 0.1 m in the surface water could not grow further because of the light limitation, although nutrients were sufficient. However, even though Z_{limf} was low, the growth of floating thalli in the surface water (–0.1 m < depth < 0 m) is not excluded, but it takes longer (Jin et al. 2018). This is also a reasonable explanation as to why the floating thalli grew rapidly only when they floated out of the Subei Shoal. Z_{limg}, the depth with a transmitted light intensity equal to $[Min\_L]_g$, was even shallower than that of $[Min\_L]_f$, i.e. <0.1 m in the majority of the Subei Shoal. This might explain why *U. prolifera* germlings easily settled on the *Porphyra* farming rafts rather than on the benthic floor.

3.4. Increase in *U. prolifera* biomass drifting northward

Floating *U. prolifera* in the Yellow Sea usually occurs at the end of April and develops into green tides from May to July (Wang et al. 2018). The distribution of nutrients and light intensity investigated in May and July actually reflects the state after biotic absorption of nutrients and biomass increase; however,

the distributions investigated in April are closer to the real state contributing to floating *U. prolifera* growth. Therefore, using the latter to calculate the biomass of *U. prolifera* forming green tide is better than the former. Solar intensity reaching the Yellow Sea is consistent throughout the late spring (Kalnay et al. 1996, Kistler et al. 2001).

The unique morphological features of bloom-forming *U. prolifera*, i.e. highly branched and hollow tubular thalli with monochromatic walls, facilitate floating on the surface water, fast nutrient uptake, and rapid growth (X. Zhang et al. 2008, Luo et al. 2012, B. Zhang et al. 2012, Zhou et al. 2015). Such a competitive edge unavoidably leads to a dramatic increase in biomass when *U. prolifera* drifts northward and to large-scale green tides in the southern sea area along the Shandong Peninsula. Considering the development of the green tide of *U. prolifera* in 2017 as an example, the entire green tide development process can be divided into 4 phases (Fig. 6): Phase A, thalli grew south of 35° N in a small coverage ratio from 19 to 24 May; Phase B, thalli drifted through the 'rapid growth zone' between 34.5° and 35.5° N from 26 May to 5 June; Phase C, thalli lingered and drifted northeastward from 6 June to 15 June; and Phase D, thalli zigzagged due to interactions between wind and current and drifted northeastward onto the coast of the Shandong Peninsula from 16 June to 10 July (Zhang 2020) (Table 3).

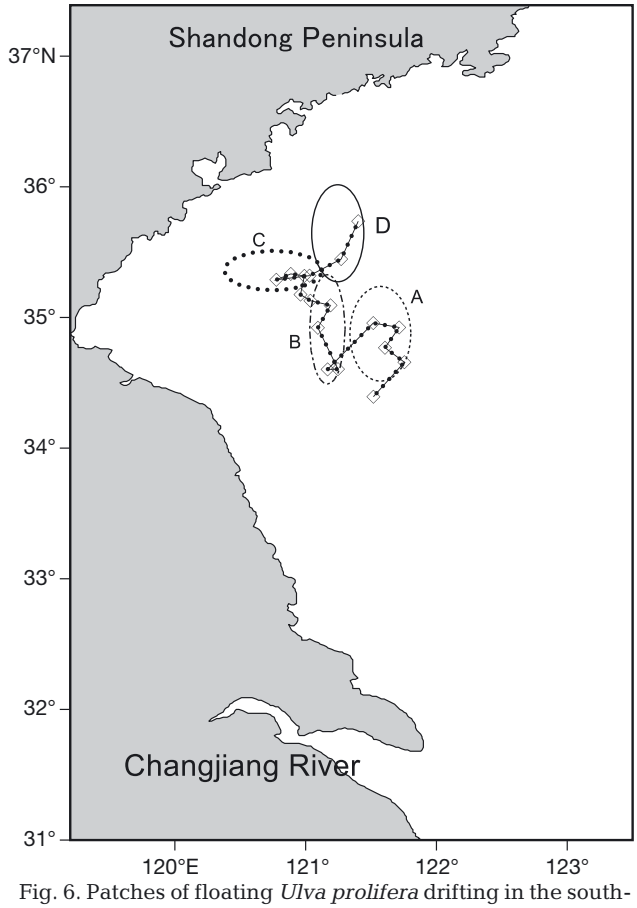

Fig. 6. Patches of floating *Ulva prolifera* drifting in the southern Yellow Sea in 2017 (solid-circle line: *U. prolifera* drifting northward; dashed line: phase A; dashed/dotted line: phase B; dotted line: phase C; solid line: phase D; see Section 3.4 for descriptions of the phases); square symbols are the central points of coverage area

Based on the distribution of BDN, TDP, ALIN, and Z_{limf}, the phased multiple increase in biomass (Mp) of *U. prolifera* was calculated using Eq. (9) (Table 3). The value of 66.91 in accumulated Mp (AcMp) calculated in the present study was very close to the value of 60.4 measured based on the area covered by *U. prolifera*. Moreover, the values of average Mp per day (AvMpd) obtained by the 2 methods were consistent with each other. Regarding the difference in AvMpd during Phase A between the 2 methods, low image recognition of current remote sensing technology resulted in an underestimation of the coverage of the smaller *U. prolifera* patches during the early phase of green tide development, which enlarged the AcMp in Phase A and thus, the AvMpd. It has been previously reported that smaller *U. prolifera* patches scattered south of 35° N cannot be identified by remote sensing (Huang et al. 2014, Guo et al. 2016, Xia 2016). AvMpd in Phase B was the closest for the 2 methods, as the largest increase (~5-fold) during this phase resulted in a reduction in other deviations. During Phase C, AvMpd from the coverage area was slightly lower than that in the present study, which can be attributed to the thickening of *U. prolifera*, with high accumulation occurring when *U. prolifera* patches floated north of 35° N and their thickness also increased to a certain extent (Zhang et al. 2013, Zhang 2020). During Phase D, the thalli began to decay and form clumps, with the AvMpd from the coverage area being slightly lower than 1. However, the AvMpd obtained from the model maintained a low rate because our model cannot be used to describe the process of decay.

During the last few decades, green tides have occurred worldwide, and many dynamic models of macroalgae have been constructed to describe the growth of macroalgae, including in Venice lagoon, the Baltic Sea, and the Avon-Heathcote Estuary (Solidoro et al. 1997, Risén et al. 2013, Ren et al. 2014, Lamb 2018), and proved promising. Light, temperature, nutrients, carbon, dissolved oxygen, grazing, and even currents are usually included in these dynamic models, making parameter verification and use difficult for environmental administrators. How-

Table 3. Comparison between multiple increases in the biomass of *Ulva prolifera* in 2017 calculated from satellite remote sensing images compared to that calculated in the present study using Eq. (9) with bioavailable dissolved nitrogen (BDN), total dissolved phosphorus (TDP), and average light intensity (ALIN). Coverage area was derived from remote sensing data (Bureau of Beihai, Ministry of Natural Resources, China). AcMp: accumulated multiple of increase in biomass; Mpd: multiple of increase in biomass per day; AvMpd: average multiple of increase in biomass per day

Phase	Satellite remote sensing images				Present study			
	Date (d-mo-yr)	Coverage area (km^2)	AcMp	AvMpd (d^{-1})	Growth time (d)	Mpd (d^{-1})	AcMp	AvMpd (d^{-1})
A	19-05-2017	5	1	1.23	1	1.20	1.20	1.17
	20-05-2017	7	1.4		1	1.23	1.49	
	21-05-2017	24	4.8		3	1.16	2.37	
	24-05-2017	17.5	3.5		2	1.11	3.08	
B	26-05-2017	34	6.8	1.19	1	1.21	3.73	1.16
	27-05-2017	75	15		1	1.17	4.36	
	28-05-2017	102	20.4		1	1.17	5.1	
	29-05-2017	105	21		3	1.22	9.48	
	01-06-2017	73	14.6		1	1.13	10.65	
	02-06-2017	143	28.6		1	1.15	12.27	
	03-06-2017	161	32.2		1	1.15	14.14	
	04-06-2017	155	31		1	1.14	15.81	
	05-06-2017	142	28.4		1	1.14	17.63	
C	06-06-2017	137	27.4	1.08	1	1.15	19.87	1.13
	07-06-2017	176	35.2		1	1.15	22.89	
	08-06-2017	175	35		1	1.14	25.96	
	09-06-2017	251	50.2		1	1.13	29.33	
	10-06-2017	240	48		1	1.14	33.17	
	11-06-2017	260	52		1	1.16	38.34	
	12-06-2017	264	52.8		1	1.16	44.39	
	13-06-2017	281	56.2		1	1.15	51.14	
	14-06-2017	284	56.8		1	1.16	59.12	
	15-06-2017	302	60.4		1	1.13	66.91	
D	16-06-2017	264	52.8	0.99	1	1.12	74.84	1.07
	17-06-2017	277	55.4		1	1.10	82.61	
	18-06-2017	255	51		1	1.11	91.34	

ever, Eq. (9) is simple and easy to understand. As a shelf-margin sea, the Yellow Sea has a strong coastal current and highly turbid seawater, which facilitate the growth of floating *U. prolifera* forming green tides (Wang et al. 2018, Wei et al. 2018). Dissolved nutrients (N and P) and light intensity became the dominant factors significantly regulating the biomass increase of floating *U. prolifera* in the south Yellow Sea. Eq. (9) only applies the 2 dominant factors to predict biomass increase, and the modeled outcomes are reliable compared with the remote sensing data.

3.5. Use of a grid to predict the multiple increase (Mp) in biomass of *U. prolifera* drifting northward

The AcMp predictions for *U. prolifera* were calculated using the Mpd (Fig. 7) and T_e (Table 3) and compared to the ratio of the coverage area from the remote sensing data. For example, the green tide of *U. prolifera* was presumed to drift northward via the middle path in 2017. The central trace of floating *U. prolifera* was presumed to be located within grids D6, E6, D5, and E5 from 19 to 25 May (Fig. 7). Mpd for the grids in which *U. prolifera* remained was (1.31 + 1.16 + 1.10)/3 d^{-1} and the corresponding *t* was 6 d. Therefore, a value of 2.84, namely $[(1.31 + 1.16 + 1.10)/3]^6$, was obtained for the AcMp of *U. prolifera* during this phase. The following central trace of *U. prolifera* drifted westerly into grids D6, D5, and E5, and then floated north into grids C5, D5, and D4, and was finally driven into grids D4, C4, and D5 for 6, 8, and 5 d, respectively (Fig. 7). Similarly, the AcMpds in these phases from 26 to 31 May, from 1 to 8 June, and from 9 to 15 June were 2.94, 3.43, and 2.07, i.e. $[(1.31 + 1.18 + 1.10)/3]^6$, $[(1.32 + 1.18 + 1.00)/3]^8$, and $[(1.00 + 1.15 + 1.32)/3]^5$, respectively. The AcMp for the total process was 59.28, which was close to that from the coverage area of *U. prolifera* (Table 3). This partly supported the reliability of Eq. (9). Only taking the main ecological factors into consideration, Eq. (9) is a simplification of *U. prolifera* growth in the southern Yellow Sea, which ignores some ecological strategies, luxury consumption and storage of nutrients, for example (Revilla & Weissing 2008, Lamb 2018). Because average biomass in the grid was calculated, luxury consumption and storage of nutrients should have less impact on the calculation of biomass than the nutrient concentration and light intensity.

In 2010, patches of *U. prolifera* drifted along the west path to the southern sea area of the Shandong Peninsula, moving through grids B5, C5, and D5, then through grids B4, C4, and D4, and finally through grids B3, C3, and D3 from early June to early July 2010. The Mpd values in these grids were 1.27, 1.15, and 1.06 d^{-1}, respectively. The corresponding T_e values were 7, 9, and 10, respectively. The predicted AcMp was calculated to be 32.9. Although the literature has reported different coverage areas of *U. prolifera* appearing on 2 June, e.g. 16 km^2 (Huang et al.

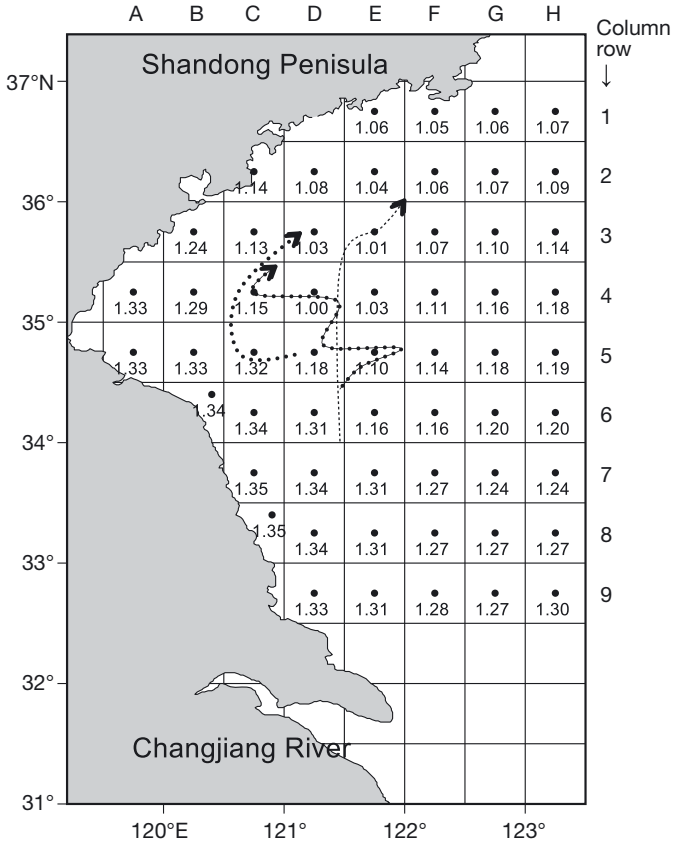

Fig. 7. Multiple of increase in biomass per day for floating *Ulva prolifera* (Mpd, d^{-1}) drifting in the southern Yellow Sea (dotted, solid-circle, and dashed curves represent centroid trace of floating *U. prolifera* through the west path, middle path, and east path [see Section 2.4], respectively, in 2010, 2017, and 2009)

2014) and 51 km^2 (Guo et al. 2016), and different maximal coverages of 530 km^2 on 10 July (Huang et al. 2014) and 1734 km^2 on 6 July (Guo et al. 2016), the AcMp calculated using the coverage area of *U. prolifera* was almost the same, with a value of 33–34, which was very close to the predicted value.

In 2009, patches of *U. prolifera* forming green tides drifted along the east path into the southern sea area of the Shandong Peninsula. The central trace of *U. prolifera* passed through grids C6, D6, and E6, moved into grids C5, D5, and E5, then through grids C4, D4, and E4, and finally through grids C3, D3, and E3 from early June to early July 2009. The Mpd values in these grids were 1.27, 1.2, 1.06, and 1.06 d^{-1}. The corresponding T_e values were estimated as 7, 9, 10, and 16 d, respectively. Thus, the AcMp was calculated to be 118.9. This predicted value was 25% lower than the AcMp (162) calculated using the coverage area of *U. prolifera* on 3 June (13 km^2) and 2 July (2100 km^2) (Huang et al. 2014), demonstrating the effectiveness of the simple prediction figure and table. Neglecting the decrease in the light intensity value when calculating the predicted value could be a possible reason for this difference. The harvest of *U. prolifera* and error in the remote sensing data might also be possible explanations for the difference in AcMp of *U. prolifera* obtained using the 2 methods. Although the difference between AcMp calculated with Mpd in the grids and that with the coverage area was large, AcMp prediction using Mpd in grids is still useful, as it can be easily obtained based on the possible drift pathway.

4. CONCLUSIONS

The calculated ALIN was strong from the head of Haizhou Bay to the open waters of the south Yellow Sea, with a value higher than 80 W m^{-2}. On the south side of 35° N, ALIN decreased gradually from north to south. The calculated $[Min\_N]_f$, $[Min\_N]_g$, $[Min\_P]_f$, and $[Min\_P]_g$ all increased with decreasing ALIN. The distribution of ALIN determined the distribution of $[Min\_N]_f$, $[Min\_N]_g$, $[Min\_P]_f$, and $[Min\_P]_g$. Moreover, [Min_N] and [Min_P] were both much larger for germlings than for floating thalli, indicating that germlings are more vulnerable to N and P limitation than thalli.

According to distributions of BDN and TDP concentrations, neither N nor P were the limiting factor for floating thalli in the majority of the study area. However, both N and P were the limiting factors for germlings of *Ulva prolifera* except in the coastal waters of Jiangsu Province in the southern Yellow Sea. Thus, floating thalli growth rather than germling growth out of the Subei Shoal contributes to a marked increase in biomass, causing green tides of *U. prolifera* in the south Yellow Sea. Z_{limf} was less than 0.1 m in most parts of the Subei Shoal, indicating that growth of floating thalli took longer but was not excluded entirely. This presented a reasonable explanation as to why the floating thalli grew rapidly only when they floated out of the Subei Shoal.

Based on the distributions of BDN, TDP, ALIN, and Z_{limf}, AcMp and AvMpd of *U. prolifera* drifting northward in 2017 were calculated using the growth function established for *U. prolifera* and compared with the AcMp obtained from the coverage area of remote sensing data. A grid figure with Mpd of *U. prolifera* was presented to predict AcMp when *U. prolifera* drifted northward via different pathways.

Acknowledgements. This study was supported by the China National Key Research and Development Program (Project No. 2016YFC1402101), the Marine Special Program of Jiangsu Province in China (Project No. JSZRHYKJ202007), the Startup Foundation for Introducing Talent of NUIST (Project No. 2020r028), and the National Key Research and Development Program of China (2019YFE0124700).

LITERATURE CITED

Baltar F, Lundin D, Palovaara J, Lekunberri I, Reinthaler T, Herndl GJ, Pinhassi J (2016) Prokaryotic responses to ammonium and organic carbon reveal alternative CO_2 fixation pathways and importance of alkaline phosphatase in the mesopelagic North Atlantic. Front Microbiol 7:1670

Chávez-Sánchez T, Piñón-Gimate A, Serviere-Zaragoza E, López-Bautista JM, Casas-Valdez M (2018) *Ulva* blooms in the southwestern Gulf of California: reproduction and biomass. Estuar Coast Shelf Sci 200:202–211

Chen Y (2015) Effects of temperature and solar radiation on the growth and nitrate reductase activity of *Ulva prolifera*. PhD dissertation, Ocean University of China, Qingdao

Chróst RJ, Overbeck J (1987) Kinetics of alkaline phosphatase activity and phosphorus availability for phytoplankton and bacterioplankton in Lake Plußsee (North German eutrophic lake). Microb Ecol 13:229–248

Ebelhar SA, Chesworth W, Paris Q (2008) Law of the minimum. In: Chesworth W (ed) Encyclopedia of soil science. Springer, Dordrecht, p 431–437

Gao G, Zhong Z, Zhou X, Xu J (2016) Changes in morphological plasticity of *Ulva prolifera* under different environmental conditions: a laboratory experiment. Harmful Algae 59:51–58

Ge R, Guo J, Yu F, Guo B (2006) Classification of vertical temperature structure and thermocline analysis in the Yellow Sea and East China Sea shelf sea areas. Adv Mar Sci 24:424–435

González-Galisteo S, Packard TT, Gómez M, Herrera A and others (2019) Calculating new production from nitrate reductase activity and light in the Peru Current upwelling. Prog Oceanogr 173:78–85

Grasshoff K, Kremling K, Ehrhardt M (eds) (2007) Methods of seawater analysis, 3rd edn. John Wiley & Sons, Hoboken, NJ

Guo W, Zhao L, Li X (2016) The interannual variation of green tide in the Yellow Sea. Haiyang Xuebao 38:36–45

He J, Shi Y, Wang Y, Shao H, Liu D (2013) Impact of temperature and nutrients on the growth of *Ulva prolifera* and *Ulva intestinalis*. Mar Sci Bull 32:573–578

Hiraoka M, Ohno M, Kawaguchi S, Yoshida G (2004) Crossing test among floating *Ulva* thalli forming 'green tide' in Japan. Hydrobiologia 512:239–245

Huang B, Ou L, Wang X, Huo W and others (2007) Alkaline phosphatase activity of phytoplankton in East China Sea coastal waters with frequent harmful algal bloom occurrences. Aquat Microb Ecol 49:195–206

Huang J, Wu L, Gao S, Li J (2014) Analysis on the interannual distribution variation of green tide in Yellow Sea. Acta Laser Biol Sin 23:572–578

Jäger CG, Diehl S, Schmidt GM (2008) Influence of water-column depth and mixing on phytoplankton biomass, community composition, and nutrients. Limnol Oceanogr 53:2361–2373

Jin S, Liu Y, Sun C, Wei X, Li H, Han Z (2018) A study of the environmental factors influencing the growth phases of *Ulva prolifera* in the southern Yellow Sea, China. Mar Pollut Bull 135:1016–1025

Jing Y (2020) Temporal and spatial distribution of amino acids and DON bioavailability in the occurrence of macroalgal blooms (*Ulva prolifera*) in the Yellow Sea. MSc thesis, Ocean University of China, Qingdao

Kalnay E, Kanamitsu M, Kistler R, Collins W and others (1996) The NCEP/NCAR 40-year reanalysis project. Bull Am Meteorol Soc 77:437–472

Kamer K, Boyle KA, Fong P (2001) Macroalgal bloom dynamics in a highly eutrophic Southern California estuary. Estuaries 24:623–635

Kapraun DF (1970) Field and cultural studies of *Ulva* and *Enteromorpha* in the vicinity of Port Aransas, Texas. Contrib Mar Sci 15:205–285

Kelble CR, Ortner PB, Hitchcock GL, Boyer JN (2005) Attenuation of photo synthetically available radiation (PAR) in Florida Bay: potential for light limitation of primary producers. Estuaries 28:560–571

Kistler R, Kalnay E, Collins W, Saha S and others (2001) The NCEP–NCAR 50-year reanalysis: monthly means CD-ROM and documentation. Bull Am Meteorol Soc 82: 247–268

Labry C, Delmas D, Youenou A, Quere J and others (2016) High alkaline phosphatase activity in phosphate replete waters: the case of two macrotidal estuaries. Limnol Oceanogr 61:1513–1529

Lalli CM, Parsons TR (1993) Biological oceanography: an introduction. Pergamon Press, Oxford

Lamb A (2018) *Ulva* spp. bloom dynamics in a hypereutrophic estuary: Jamaica Bay, New York. PhD dissertation, City University of New York

Lang E (1924) The law of the soil. In: Spillman WJ, Lang E (eds) The law of diminishing returns. World Book Company, New York, NY, p 233–235

Li H (2015) Relationship between nutrients and the occurrence of macroalgal blooms in the Yellow Sea. PhD dissertation, Ocean University of China, Qingdao

Lin A, Shen S, Wang J, Yan B (2008) Reproduction diversity of *Enteromorpha prolifera*. J Integr Plant Biol 50:622–629

Lindenschmidt KE, Chorus I (1998) The effect of water column mixing on phytoplankton succession, diversity and similarity. J Plankton Res 20:1927–1951

Liu D, Keesing JK, Xing Q, Shi P (2009) World's largest macroalgal bloom caused by expansion of seaweed aquaculture in China. Mar Pollut Bull 58:888–895

Lorenzen CJ (1972) Extinction of light in the ocean by phytoplankton. ICES J Mar Sci 34:262–267

Luo MB, Liu F, Xu ZL (2012) Growth and nutrient uptake capacity of two co-occurring species, *Ulva prolifera* and *Ulva linza*. Aquat Bot 100:18–24

McLaughlin K, Sohm JA, Cutter GA, Lomas MW, Paytan A (2013) Phosphorus cycling in the Sargasso Sea: investigation using the oxygen isotopic composition of phosphate, enzyme-labeled fluorescence, and turnover times. Global Biogeochem Cycles 27:375–387

Nausch M, Nausch G (2006) Bioavailability of dissolved organic phosphorus in the Baltic Sea. Mar Ecol Prog Ser 321:9–17

Odum EP, Barrett GW (2005) Fundamentals of ecology. Saunders Company, Philadelphia, PA

Ren JS, Barr NG, Scheuer K, Schiel DR, Zeldis J (2014) A dynamic growth model of macroalgae: application in an

estuary recovering from treated wastewater and earthquake-driven eutrophication. Estuar Coast Shelf Sci 148:59–69

Revilla T, Weissing FJ (2008) Nonequilibrium coexistence in a competition model with nutrient storage. Ecology 89: 865–877

Risén E, Pechsiri JS, Malmström ME, Brandt N, Gröndahl F (2013) Natural resource potential of macroalgae harvesting in the Baltic Sea — case study Trelleborg, Sweden. In: Moksness E, Dahland E, Støttrup J (eds) Global challenges in integrated coastal zone management. John Wiley & Sons, Chichester, p 71-84

Shelford VE (1913) The reactions of certain animals to gradients of evaporating power of air. A study in experimental ecology. Biol Bull (Woods Hole) 25:79–120

Solidoro C, Pecenik G, Pastres R, Franco D, Dejak C (1997) Modelling macroalgae (*Ulva rigida*) in the Venice lagoon: model structure identification and first parameters estimation. Ecol Modell 94:191–206

Song W, Wang Z, Li Y, Han H, Zhang X (2019) Tracking the original source of the green tides in the Bohai Sea, China. Estuar Coast Shelf Sci 219:354–362

Sun K, Li R, Li Y, Xin M and others (2015) Responses of *Ulva prolifera* to short-term nutrient enrichment under light and dark conditions. Estuar Coast Shelf Sci 163:56–62

Touchette BW, Burkholder JM (2000) Review of nitrogen and phosphorus metabolism in seagrasses. J Exp Mar Biol Ecol 250:133–167

Valiela I, McClelland J, Hauxwell J, Behr PJ, Hersh D, Foreman K (1997) Macroalgal blooms in shallow estuaries: controls and ecophysiological and ecosystem consequences. Limnol Oceanogr 42:1105–1118

von Bertalanffy L (1951) Metabolic types and growth types. Am Nat 85:111–117

Wang C, Su R, Guo L, Yang B and others (2019) Nutrient absorption by *Ulva prolifera* and the growth mechanism leading to green-tides. Estuar Coast Shelf Sci 227: 106329–106339

Wang C, Jiao X, Zhang Y, Zhang L, Xu H (2020) A light-limited growth model considering the nutrient effect for improved understanding and prevention of macroalgae bloom. Environ Sci Pollut Res 27:12405–12413

Wang K, Ma C, Chen W, Zhang F (2009) Error analysis for gate centroid tracking algorithm of infrared imaging. J Appl Opt 30:353–356

Wang Z, Xiao J, Fan S, Li Y, Liu X, Liu D (2015) Who made the world's largest green tide in China? An integrated study on the initiation and early development of the green tide in Yellow Sea. Limnol Oceanogr 60: 1105–1117

Wang Z, Fu M, Xiao J, Zhang X, Song W (2018) Progress on the study of the Yellow Sea green tides caused by *Ulva prolifera*. Haiyang Xuebao 40:1–13

Wei Q, Wang B, Yao Q, Fu M, Sun J, Xu B, Yu Z (2018) Hydro-biogeochemical processes and their implications for *Ulva prolifera* blooms and expansion in the world's largest green tide occurrence region (Yellow Sea, China). Sci Total Environ 645:257–266

Wu T (2013) Preliminary study on the influence of nutrients on the growth of *Ulva prolifera* and its absorption of different nitrogen species. MSc thesis, Ocean University of China, Qingdao

Xia S (2016) Distribution and driving mechanism of the drift velocity of *Ulva prolifera* in the Yellow Sea based on remote sensing. MSc thesis, Nanjing University

Xiu B, Liang SK, He XL, Wang XK, Cui ZG, Jiang ZJ (2019) Bioavailability of dissolved organic nitrogen and its uptake by *Ulva prolifera*: implications in the outbreak of a green bloom off the coast of Qingdao, China. Mar Pollut Bull 140:563–572

Yi L, Zhang S, Yin Y (2010) Influence of environmental hydro-meteorological conditions to *Enteromorpha prolifera* blooms in Yellow Sea, 2009. Period Ocean Univ China 10:18–26

Zhang BX, Wang JZ, Wang YF, Wang L, Shen SD (2012) Growth and reproduction of the green macroalga *Ulva prolifera*. Acta Ecol Sin 32:421–430

Zhang H (2020) The relationship between development phases (logistic) of floating *Ulva prolifera* green tides and nutrients and environmental variables in the southern Yellow Sea, China. PhD dissertation, Ocean University of China, Qingdao

Zhang H, Su R, Shi X, Zhang C, Yin H, Zhou Y, Wang G (2020) Role of nutrients in the development of floating green tides in the southern Yellow Sea, China, in 2017. Mar Pollut Bull 156:111197

Zhang JH, Huo YZ, Zhang ZL, Yu KF and others (2013) Variations of morphology and photosynthetic performances of *Ulva prolifera* during the whole green tide blooming process in the Yellow Sea. Mar Environ Res 92:35–42

Zhang X, Mao Y, Zhuang Z, Liu S, Wang Q, Ye N (2008) Morphological characteristics and molecular phylogenetic analysis of green tide *Enteromorpha* sp. occurred in the Yellow Sea. J Fish Sci China 15:822–829

Zhang Y, Yin M (2007) Phosphorus cycling in the upper ocean of the East China Sea using natural ^{32}P and ^{33}P. Acta Oceanol Sin 29:49–57

Zhou MJ, Liu DY, Anderson DM, Valiela I (2015) Introduction to the Special Issue on green tides in the Yellow Sea. Estuar Coast Shelf Sci 163:3–8

Editorial responsibility: Pei-Yuan Qian Kowloon, Hong Kong SAR
Reviewed by: T. A Nelson, C. Gobler and 1 anonymous referee

Submitted: January 14, 2021
Accepted: June 7, 2021
Proofs received from author(s): July 27, 2021